Available online at www.sciencedirect.com
SCIENCE DIRECT®
Journal of Computational Physics 189 (2003) 527–538
JOURNAL OF COMPUTATIONAL PHYSICS
www.elsevier.com/locate/jcp

Comparison of splitting algorithms for the rigid body

Francesco Fassò

Dipartimento di Matematica Pura e Applicata, Università di Padova, Via G. Belzoni 7, 35131 Padova, Italy

Received 6 September 2002; received in revised form 19 February 2003; accepted 8 April 2003

Abstract

We compare several different second-order splitting algorithms for the asymmetric rigid body, with the aim of determining which one produces the smallest energy error for a given rigid body, namely, for given moments of inertia. The investigation is based on the analysis of the dominant term of the modified Hamiltonian and indicates that different algorithms can produce energy errors which differ by several orders of magnitude. As a byproduct of this analysis we remark that, for the special case of a flat rigid body with moments of inertia proportional to $(1, 0.75, 0.25)$, one of the considered algorithms is in fact of order four.

PACS: 65P10; 70-08

Keywords: Symplectic integrators; Splitting methods; Numerical integration of rigid bodies

1. Introduction

(A) A variety of numerical algorithms have been developed for the integration of the equations of motion of the rigid body. Nowadays, in areas such as Celestial Mechanics and Molecular Dynamics, there is special interest for symplectic algorithms and, among them, for splitting algorithms. The purpose of this article is to compare a few second-order splitting algorithms for the asymmetric rigid body, i.e., the rigid body with three different moments of inertia I_1, I_2, and I_3. Even though the interesting case is that of a body subject to external forces and with no fixed point, we focus the analysis on the case of a rigid body with a fixed point and no external forces—the so-called "Euler–Poinsot" system. The reason is that, ordinarily, an algorithm for the Euler–Poinsot flow is used in splitted algorithms for the general case and hence its quality affects the quality of the overall algorithm. We shall come back on this point in Section 5.

If the three moments of inertia are all different, the computation of the flow of the Euler–Poinsot system requires the evaluation of a few special functions and the solution of a time-dependent ordinary differential equation (see e.g. [6]). It would be of great interest to possess an efficient numerical algorithm for

E-mail address: fasso@math.unipd.it.
URL: www.math.unipd./~fasso.

0021-9991/$ - see front matter
doi:10.1016/S0021-9991(03)00232-8

performing this computation exactly (that is, to machine precision), but there appear to be difficulties related, in particular, to the integration of the time-dependent ODE. Therefore, approximate algorithms are usually employed.

Splitting algorithms for a Hamiltonian system rely on the possibility of writing the Hamiltonian K as the sum of two or more functions, the Hamiltonian flows of which can be computed exactly (and efficiently). If $K = F_1 + F_2$ and if Φ_h^F denotes the map at time h of the flow of a Hamiltonian F, then the so-called Strang splitting $\Phi_{h/2}^{F_2} \circ \Phi_h^{F_1} \circ \Phi_{h/2}^{F_2}$ is a second-order algorithm for Φ_h^K:

$$\Phi_h^K = \Phi_{h/2}^{F_2} \circ \Phi_h^{F_1} \circ \Phi_{h/2}^{F_2} + \mathcal{O}(h^3).$$

Similarly, if $K = F_1 + F_2 + F_3$, then

$$\Phi_h^K = \Phi_{h/2}^{F_3} \circ \Phi_{h/2}^{F_2} \circ \Phi_h^{F_1} \circ \Phi_{h/2}^{F_2} \circ \Phi_{h/2}^{F_3} + \mathcal{O}(h^3).$$

These algorithms are obviously symplectic and exhibit the typical good properties of symplectic algorithms, including good energy conservation (see [5] for general background on these algorithms).

To our knowledge, the use of splitting algorithms for rigid body dynamics was proposed by Touma and Wisdom [11], McLachlan [8] and Reich [10]. The basis of the method is easily explained. The Hamiltonian K of the Euler–Poinsot system is the kinetic energy. Denoting by $M = (M_1, M_2, M_3)$ the angular momentum vector in the body base, the axes of which are the principal axes of inertia of the body, one has

$$K(M; I_1, I_2, I_3) = \frac{M_1^2}{2I_1} + \frac{M_2^2}{2I_2} + \frac{M_3^2}{2I_3} \tag{1}$$

(see e.g. [1,2,7] for all the necessary background on rigid body dynamics). Now, while it is difficult to compute exactly the flow of K, it is easy (and efficient) to compute exactly the flows of the three "rotational" Hamiltonians

$$R_j(M; I_j) = \frac{M_j^2}{2I_j}, \quad j = 1, 2, 3 \tag{2}$$

and the flow of the Hamiltonian S of the *symmetric* Euler–Poinsot system, which has two moments of inertia equal, say $I_1 = I_2$,

$$S(M; I_2, I_3) = \frac{M_1^2 + M_2^2}{2I_2} + \frac{M_3^2}{2I_3} \tag{3}$$

(see the Remark). By suitably combining these flows, one can construct a number of second-order approximations to Φ^K. A few natural choices considered in the above-mentioned references, or simple variants of them, are the following:

(i) The *Symmetric + Rotation* ("SR") splitting

$$\Psi_h^{\mathrm{SR}} = \Phi_{h/2}^R \circ \Phi_h^S \circ \Phi_{h/2}^R$$

obtained by decomposing K as the sum of a symmetric rigid body Hamiltonian and of a suitable rotational term: $K(M; I_1, I_2, I_3) = S(M; I_2, I_3) + R(M; I_1, I_2)$ for S as in (3) and

$$R(M; I_1, I_2) = \frac{1}{2}\left(\frac{1}{I_1} - \frac{1}{I_2}\right) M_1^2.$$

(ii) The *Rotation + Symmetric* ("RS") splitting

$$\Psi_h^{\mathrm{RS}} = \Phi_{h/2}^S \circ \Phi_h^R \circ \Phi_{h/2}^S$$

which differs from the previous one just in the ordering. Of course, these two algorithms are "conjugate", that is

$$\Psi_h^{\mathrm{RS}} = \mathscr{C} \circ \Psi_h^{\mathrm{SR}} \circ \mathscr{C}^{-1}, \quad \mathscr{C} = \Phi_{h/2}^{S} \circ \Phi_{h/2}^{R}.$$

Therefore, by iteration, they produce algorithms with the same properties—actually, essentially the same algorithm: $(\Psi_h^{\mathrm{RS}})^n = \mathscr{C} \circ (\Psi_h^{\mathrm{SR}})^n \circ \mathscr{C}^{-1}$ (see [5] for the properties of conjugate algorithms). However, conjugacy may be lost if these algorithms are used for constructing splitting algorithms for a rigid body with external forces, see Section 5. Hence, we consider them separately.

(iii) The *Three Rotations* ("3R") splitting

$$\Psi_h^{\mathrm{3R}} = \Phi_{h/2}^{R_3} \circ \Phi_{h/2}^{R_2} \circ \Phi_h^{R_1} \circ \Phi_{h/2}^{R_2} \circ \Phi_{h/2}^{R_3}$$

which is based on the decomposition of K as the sum $R_1 + R_2 + R_3$ of the three rotational terms as in (2). Some pairs of these algorithms are conjugate, e.g., those with orderings $(I_{\min}, I_{\mathrm{mid}}, I_{\max})$ and $(I_{\max}, I_{\mathrm{mid}}, I_{\min})$, but here too conjugacy may be lost if an external potential is added.

Note that for a given body, namely for given moments of inertia $I_{\min} < I_{\mathrm{mid}} < I_{\max}$, there are six different algorithms of each type SR, RS and 3R, which are obtained by choosing (I_1, I_2, I_3) as all possible permutations of $(I_{\min}, I_{\mathrm{mid}}, I_{\max})$.

Remark. These algorithms have been implemented in a variety of ways. In all cases, computing Φ_h^S and $\Phi_h^{R_j}$ requires the evaluation of only four and, respectively, two trigonometric functions, besides a small number of algebraic operations. Touma and Wisdom [11], McLachlan [8] and Reich [10] resorted to the left trivialization of $T^*\mathrm{SO}(3)$. This leads to a "Lie–Poisson" algorithm for solving the Euler equations for the angular momentum vector in the body base and to an algorithm for either a rotational matrix or for a unit quaternion (in fact, the use of quaternions has some advantages). We refer the reader to [4] for an exhaustive treatment of the problem and for the implementation details. More recently, an implementation which uses two charts with Euler angles, so as to avoid the singularity of these coordinates, has also been developed [3]. However, such an implementation is not as simple as the quaternionic one and, in the author's experience, slightly less efficient.

(B) The purpose of this article is to compare the above splitting algorithms, with the aim of determining whether they produce significantly different errors in the energy conservation and, in such a case, which one is the "best" one, in the sense that it produces the smallest energy error for given rigid body, namely, for given moments of inertia $(I_{\min}, I_{\mathrm{mid}}, I_{\max})$. Of course, it is expected that some SR or RS algorithm performs better for nearly symmetric bodies but, as it will be seen, even in this limit case it is a priori not clear which is the best one.

Following a well-established procedure, see e.g. [9], we base the investigation on the fact that, as many other symplectic algorithms, any splitting algorithm Ψ_h for Φ_h^K possesses a "modified Hamiltonian"

$$\tilde{K} = K + \frac{h^2}{12}\tilde{K}_2 + \mathscr{O}(h^4)$$

such that

$$\Psi_h = \Phi_h^{\tilde{K}} + \mathscr{O}(\exp(-1/h)).$$

Hence, up to quantities of the order of $\exp(-1/h)$, the energy error is given by

$$K - \tilde{K} = \frac{h^2}{12}\tilde{K}_2 + \mathscr{O}(h^4)$$

(see e.g. [5] for details and references). For small step sizes we can restrict the attention to the leading term $(h^2/12)\tilde{K}_2$ and thus compare the functions $|\tilde{K}_2^{\mathrm{SR}}(M;I)|$, $|\tilde{K}_2^{\mathrm{RS}}(M;I)|$ and $|\tilde{K}_2^{\mathrm{3R}}(M;I)|$ for all possible permutations of the three moments of inertia. We shall define as "best" algorithm for given $I=(I_{\min},I_{\mathrm{mid}},I_{\max})$ the one for which such a leading term, as a function of M, has the smallest maximum. Some limitations implicit to this approach are discussed in Section 5.

This analysis demonstrates that the choice of the algorithm can be very important since it can (and typically does) affect the energy error by a factor 10 or 100, or more. Therefore, for practical purposes, it is important to possess an a priori knowledge of the "best" algorithm as a function of the moments of inertia. As we shall see, the two algorithms SR and RS, with appropriate orderings of $I_{\min},I_{\mathrm{mid}},I_{\max}$, are equivalent at the leading order considered here. In the space of moments of inertia there are of course regions where the best algorithm is any of these two, with an appropriate (but not a priori obvious) ordering. However, there is also a region where the best algorithm is 3R with ordering $(I_{\max},I_{\mathrm{mid}},I_{\min})$. Interestingly, this is related to the fact that, as we shall point out, the function $\tilde{K}_2^{\mathrm{3R}}(M;I_{\max},I_{\mathrm{mid}},I_{\min})$ vanishes for a flat body with moments of inertia proportional to $(4,3,1)$, so that such a 3R splitting algorithm is in such a case a fourth-order algorithm and obviously outperforms all others.

2. The modified Hamiltonians

It is a well-known fact that the leading term $\tilde{K}_2$ of the modified Hamiltonian of the map $\Phi_{h/2}^{F_2}\circ\Phi_h^{F_1}\circ\Phi_{h/2}^{F_2}$ is

$$\frac{h^2}{12}\left\{F_1+\frac{F_2}{2},\{F_1,F_2\}\right\},$$

where $\{,\}$ denote the Poisson brackets, see e.g. [5]. One immediately deduces from here that the leading term of the modified Hamiltonian of the map $\Phi_{h/2}^{F_3}\circ\Phi_{h/2}^{F_2}\circ\Phi_h^{F_1}\circ\Phi_{h/2}^{F_2}\circ\Phi_{h/2}^{F_3}$ is

$$\frac{h^2}{12}\left[\left\{F_1+\frac{F_2}{2},\{F_1,F_2\}\right\}+\left\{F_1+F_2+\frac{F_3}{2},\{F_1+F_2,F_3\}\right\}\right]. \tag{4}$$

Specializing to the rigid body algorithms introduced before, and using $\{M_1,M_2\}=M_3$ etc., we obtain

$$\tilde{K}_2^{\mathrm{SR}}=\frac{I_1-I_2}{I_1I_2}\frac{I_2-I_3}{I_2I_3}\left[\frac{I_2-I_3}{I_2I_3}M_3^2\left(M_1^2-M_2^2\right)-\frac{I_1-I_2}{2I_1I_2}M_1^2\left(M_2^2-M_3^2\right)\right], \tag{5}$$

$$\tilde{K}_2^{\mathrm{RS}}=-\frac{I_1-I_2}{I_1I_2}\frac{I_2-I_3}{I_2I_3}\left[\frac{I_1-I_2}{I_1I_2}M_1^2\left(M_3^2-M_2^2\right)-\frac{I_2-I_3}{2I_2I_3}M_3^2\left(M_2^2-M_1^2\right)\right], \tag{6}$$

$$\begin{aligned}\tilde{K}_2^{\mathrm{3R}}=&\frac{1}{I_1I_2}\left[\frac{M_1^2}{I_1}\left(M_3^2-M_2^2\right)+\frac{M_2^2}{2I_2}\left(M_1^2-M_3^2\right)\right]+\frac{I_1-I_2}{I_1I_2I_3}\left[\frac{M_1^2}{I_1}\left(M_3^2-M_2^2\right)+\frac{M_2^2}{I_2}\left(M_1^2-M_3^2\right)\right.\\&\left.+\frac{M_3^2}{2I_3}\left(M_2^2-M_1^2\right)\right].\end{aligned} \tag{7}$$

For the present analysis, we have in mind situations in which the algorithm is applied to the integration of the motion of a rigid body without an a priori knowledge of the position of its angular momentum vector relative to the body—a typical situation in presence of strong interactions. Therefore, we measure the quality of an algorithm by the maximum (relative) energy error over all values of M.

Since the quadratic terms $\tilde{K}_2^{\mathrm{RS}}$, $\tilde{K}_2^{\mathrm{SR}}$ and $\tilde{K}_2^{3\mathrm{R}}$ are homogeneous polynomials of degree four in $M = (M_1, M_2, M_3)$, we can restrict the analysis to the sphere $\|M\| = 1$. In fact, by symmetry, all computations can be further restricted to the first octant $M_1 \geqslant 0$, $M_2 \geqslant 0$, $M_3 \geqslant 0$ of the unit sphere, but to keep the notation simple we shall not indicate this restriction. Thus, for each $I = (I_1, I_2, I_3)$ we compute the three numbers

$$\Delta^j(I) = \max_{\|M\|=1} \left|\tilde{K}_2^j(M; I)\right|, \quad j = \mathrm{SR}, \mathrm{RS}, 3\mathrm{R}.$$

Of course, for a given rigid body with moments of inertia $I = (I_{\min}, I_{\mathrm{mid}}, I_{\max})$ we must consider all 18 algorithms corresponding to the six permutations $\sigma(I)$ of the three moments of inertia. Thus, we define as "best algorithm" the one which attains

$$\Delta_{\mathrm{best}}(I) = \min_{\sigma(I)} \min_{j=\mathrm{SR},\mathrm{RS},3\mathrm{R}} \Delta^j(I).$$

Note however that $\tilde{K}_2^{\mathrm{SR}}(M_1, M_2, M_3; I_1, I_2, I_3) = -\tilde{K}_2^{\mathrm{RS}}(M_3, M_2, M_1; I_3, I_2, I_1)$, so that

$$\min_{\sigma(I)} \Delta^{\mathrm{RS}}(I) = \min_{\sigma(I)} \Delta^{\mathrm{SR}}(I).$$

Hence we need only consider the six SR and the six 3R algorithms. (Within this approach, the "best" SR and the "best" RS algorithms cannot be distinguished. They might nevertheless perform differently for given values of M.)

The polynomials $\tilde{K}_2^{\mathrm{SR}}$ and $\tilde{K}_2^{3\mathrm{R}}$ have the form

$$p(M) = 4\left(c_1 M_2^2 M_3^2 + c_2 M_3^2 M_1^2 + c_3 M_1^2 M_2^2\right) \tag{8}$$

for certain coefficients c_1, c_2, c_3 which depend on the moments of inertia. A simple argument given in Appendix A shows that

$$\max_{\|M\|=1} |p(M)| = \max\left(|c_1|, |c_2|, |c_3|, \left|\frac{4c_1c_2c_3}{c_1^2 + c_2^2 + c_3^2 - 2c_1c_2 - 2c_2c_3 - 2c_1c_3}\right|\right) \tag{9}$$

if c_1, c_2, c_3 are all nonzero and if the three numbers $(c_2 + c_3 - c_1)c_2c_3$, $(c_3 + c_1 - c_2)c_3c_1$, $(c_1 + c_2 - c_3)c_1c_2$ are either all positive or all negative, while otherwise

$$\max_{\|M\|=1} |p(M)| = \max(|c_1|, |c_2|, |c_3|). \tag{10}$$

Thus, the determination of the "best algorithm" for given I reduces to the evaluation of just three or four numbers for each type of algorithm and for each permutation of I. (As it turns out, the maximum is always $|c_{\mathrm{mid}}|$ for the SR algorithms and either $|c_1|$ or $|c_2|$ or $|c_3|$ for the 3R's.)

3. Special cases

If all three coefficients c_1, c_2, c_3 vanish, then the quadratic term of the modified Hamiltonian vanishes identically and the algorithm is of order four or higher. This possibility clearly deserves investigation.

From (5) and (6) one sees that $\tilde{K}_2^{\mathrm{SR}}(M; I_1, I_2, I_3)$ and $\tilde{K}_2^{\mathrm{RS}}(M; I_1, I_2, I_3)$ vanish if and only if either $I_1 = I_2$ or $I_2 = I_3$. The first case is obvious: the rotational Hamiltonian $R(M; I_1, I_2)$ vanishes when $I_1 = I_2$, so that the SR splitting reduces to the exact flow of a symmetric Euler–Poinsot system with moments of inertia (I_1, I_1, I_3):

$$\Phi_h^{K(M;I_1,I_1,I_3)} = \Psi_h^{\mathrm{SR}} \quad \text{if } I_1 = I_2.$$

Remarkably, the same happens also when $I_2 = I_3$:

$$\Phi_h^{K(M;I_1,I_3,I_3)} = \Psi_h^{\mathrm{SR}} \quad \text{if } I_2 = I_3.$$

The fact is that the two functions

$$S(M;I_3,I_3) = \frac{M_1^2 + M_2^2 + M_3^2}{2I_3} \quad \text{and} \quad R(M;I_1,I_3) = \frac{1}{2}\left(\frac{1}{I_1} - \frac{1}{I_3}\right)M_1^2.$$

Poisson commute and their sum is the Hamiltonian $K(M;I_1,I_3,I_3)$. Therefore, for $I_2 = I_3$, the map $\Psi_h^{\mathrm{SR}} = \Phi_{h/2}^R \circ \Phi_h^S \circ \Phi_{h/2}^R = \Phi_h^{S+R} = \Phi_h^{K(M;I_1,I_3,I_3)}$ is the (exact) flow of the symmetric Euler–Poinsot system.

From (7) one sees that the quadratic term $\tilde{K}_2^{3\mathrm{R}}(M;I_1,I_2,I_3)$ of the 3R splitting vanishes if and only if

$$I_1 = 4I_3, \quad I_2 = 3I_3.$$

This implies that *the 3R splitting with ordering* $(I_{\max}, I_{\mathrm{mid}}, I_{\min})$ *is an algorithm of order four for a rigid body with moments of inertia proportional to* $(1,3,4)$. We checked numerically that the algorithm is not of higher order.

Remark. Since the 3R splitting with ordering $(I_{\max}, I_{\mathrm{mid}}, I_{\min})$ is conjugate to that with ordering $(I_{\min}, I_{\mathrm{mid}}, I_{\max})$, it follows that the latter, even if of order two has in fact "effective order" four. (See [5] for the notion of effective order.) However, this property is lost together with the conjugacy, if an external potential is added (see Section 5).

4. Results

Since $\tilde{K}_2^{\mathrm{SR}}$ and $\tilde{K}_2^{3\mathrm{R}}$ are homogeneous in (I_1,I_2,I_3), we can normalize to one the largest moment of inertia—or equivalently parameterize the results with the ratios $(x,y) = (I_{\min}/I_{\max}, I_{\mathrm{mid}}/I_{\max})$. These two ratios take value in the triangle

$$\mathscr{T} = \{(x,y) \in \mathbb{R}^2 : 0 < 1 - y \leqslant x < y < 1\},$$

where the condition $x + y \geqslant 1$ is due to the well-known fact that the sum of any two moments of inertia of a rigid body is larger than the third one and equals it for flat bodies (see e.g. [2]). Note that for each point $(x,y) \in \mathscr{T}$ there exists a rigid body with moments of inertia $(x,y,1)$. (This is demonstrated by three points of unit mass positioned on three orthogonal axes at suitable distances from the origin.) The three lines forming the triangle $\mathscr{T}$ correspond to the oblate symmetric bodies ($x = y$), to the prolate symmetric bodies ($y = 1$) and to the flat bodies ($x + y = 1$).

The results of our analysis are reported in the figures, which were constructed by numerically evaluating the coefficients c_1, c_2, c_3 at about 50,000 points in the triangle $\mathscr{T}$.

Fig. 1 indicates the type and the ordering of the "best" algorithm. As expected, there is a region adjacent the symmetric bodies where the best algorithm is one of the SR. The ordering of such a best algorithm is $(I_{\max}, I_{\mathrm{mid}}, I_{\min})$ near the oblate bodies and $(I_{\min}, I_{\mathrm{mid}}, I_{\max})$ near the prolate ones. However, there is also a smaller region, adjoining part of the flat bodies, where the best algorithm is 3R with ordering $(I_{\max}, I_{\mathrm{mid}}, I_{\min})$. The curve dividing the various regions are specified in Appendix B.

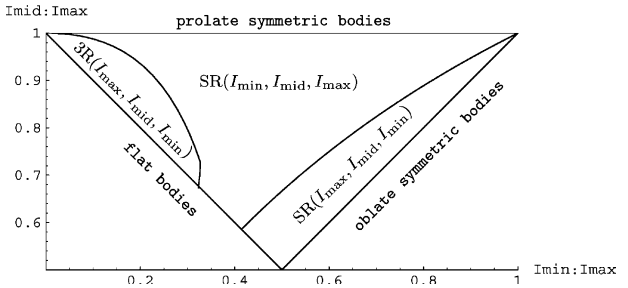

Fig. 1. The "best algorithm" as a function of the ratios $(I_{\min}/I_{\max}, I_{\mathrm{mid}}/I_{\max})$ of the moments of inertia.

Remark. At first sight, the orderings of the two "best" SR algorithms might appear strange. Consider for instance the region near the prolate symmetric bodies, where $I_{\mathrm{mid}} \approx I_{\max}$. One would expect that the best algorithm for such bodies should be the one which, in the limit $I_{\mathrm{mid}} = I_{\max}$, reduces to the exact flow of the symmetric rigid body. However, as we have seen in Section 3, the SR algorithm reduces to the exact symmetric flow in two different ways: we can either choose

$$I_1 = I_{\max}, \quad I_2 = I_{\mathrm{mid}}, \quad I_3 = I_{\min}$$

and take the limit $I_2 \to I_1$ (so that $R \to 0$) or choose instead

$$I_1 = I_{\min}, \quad I_2 = I_{\mathrm{mid}}, \quad I_3 = I_{\max}$$

and take the limit $I_2 \to I_3$. It is the latter algorithm which produces the best approximation to the flow of nearly symmetric bodies.

Fig. 2 compares the "best" algorithm with the "worst" one by plotting the ratio

$$r_{b-w}(I) := \frac{\Delta_{\mathrm{best}}(I)}{\Delta_{\mathrm{worst}}(I)},$$

where

$$\Delta_{\mathrm{worst}}(I) = \max\left[\max_{\sigma(I)} \Delta^{\mathrm{SR}}(I), \max_{\sigma(I)} \Delta^{3\mathrm{R}}(I)\right].$$

Note that $r_{b-w}(I)$ is everywhere smaller than 0.1, and in fact much smaller in some subregions. Of course, r_{b-w} tends to zero as one approaches the two lines $y = x$ and $y = 1$ corresponding to symmetric bodies, since for a symmetric body the SR algorithm with the appropriate ordering reduces to the exact flow and has therefore no energy error. The ratio $r_{b-w}(I)$ vanishes also at $(x, y) = (0.25, 0.75)$, due to the fact that one of

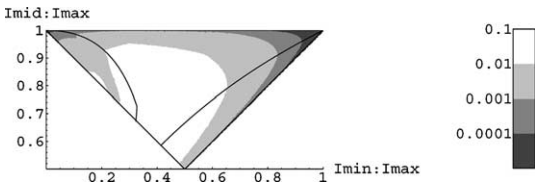

Fig. 2. Logarithmic contour plot of the ratio $\Delta_{\mathrm{best}}/\Delta_{\mathrm{worst}}$ (in the darkest region, the ratio assumes values $<10^{-4}$).

the 3R algorithm is there of order four, but the region near such a point where r_{b-w} is very small (in fact, smaller than 0.001) is very small and is not visible in the picture.

In order to obtain a clearer picture of the importance of properly chosing the algorithm, Fig. 3 compares the best algorithm to the "second-best" algorithm. As one sees, the first two best algorithms generally perform comparably, with the ratio $r_{b-2b} = \Delta_{\text{best}}/\Delta_{\text{second-best}}$ larger than 0.9 in a large region, except near $(0.25, 0.75)$ where the best algorithm is of order four and the second-best algorithm is only of order two.

The behaviour on the line of flat bodies is investigated further in Fig. 4, which plots the two ratios r_{b-w} and r_{b-2b} as a function of $I_{\min}/I_{\max}$. It is manifest that both these quantities vanish at $I_{\min}/I_{\max} = 0.25$.

Just as an example, consider the water molecule. This is a flat body with moments of inertia proportional to $(0.345, 0.653, 1)$. From Fig. 1 one deduces that the best algorithm for the water molecule is SR with ordering $(I_{\min}, I_{\text{mid}}, I_{\max})$. However, Fig. 3 indicates that the second-best algorithm performs comparably to the best one. The values of the maximum error for each algorithm are thus reported in Table 1. One sees that the best SR algorithm has an energy error over ten times smaller than the worst algorithm, but just 1.2 times smaller than the second-best SR and 1.5 times smaller than the best 3R. The latter fact is likely related to the fact that the water molecule lies nearby the border of the region where the best algorithm is of type 3R. However, the overall impression is that, a priori, it is not obvious at all which is the best choice.

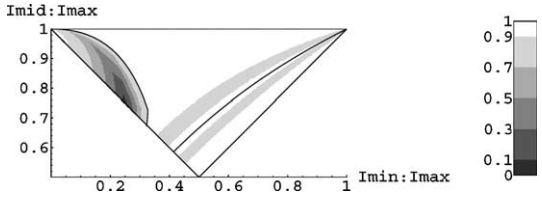

Fig. 3. Contour plot of the ratio $\Delta_{\text{best}}/\Delta_{\text{second-best}}$.

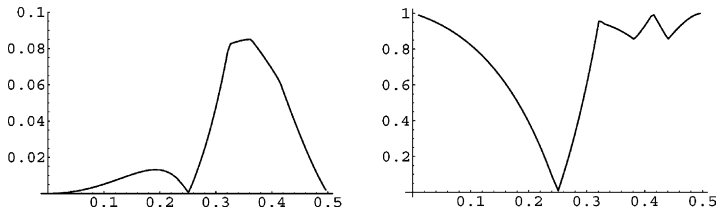

Fig. 4. The ratios $\Delta_{\text{best}}/\Delta_{\text{worst}}$ (left) and $\Delta_{\text{best}}/\Delta_{\text{second-best}}$ (right) for flat bodies.

Table 1
Energy error for the water molecule

(I_1, I_2, I_3)	$\Delta^{\text{SR}}(I)$	$\Delta^{\text{3R}}(I)$
$(I_{\min}, I_{\text{mid}}, I_{\max})$	**0.22**	2.37
$(I_{\min}, I_{\max}, I_{\text{mid}})$	0.23	0.55
$(I_{\text{mid}}, I_{\min}, I_{\max})$	1.19	2.39
$(I_{\max}, I_{\min}, I_{\text{mid}})$	0.47	0.55
$(I_{\text{mid}}, I_{\max}, I_{\min})$	0.85	**2.56**
$(I_{\max}, I_{\text{mid}}, I_{\min})$	0.29	0.33

5. Conclusions

The foregoing analysis shows that, when energy conservation is an issue, a careful choice of the algorithm can produce significant benefits. Within the class of second-order algorithms considered here, the energy error may vary by several orders of magnitudes. Fig. 1 gives a simple receipt for choosing, among these algorithms, that with the best energy conservation for given rigid body. For a full appreciation of this result we should add that the considered algorithms have all comparable speeds. As we have already mentioned, they all require the evaluation of six trigonometric functions at each time step, plus a number of algebraic operations. In fact, 3R requires fewer operations than the other two and is therefore slightly faster—about 10%, with the implementations used by the author. This difference in speed seems to be unimportant: if energy conservation is the factor which determines the size of the time step, then the energy error dominates the integration times.

We have necessarily restricted the attention to a few second-order algorithms for the Euler–Poinsot system, focusing on those which appear to have received more attention. However, other second-order splittings are conceivable and it is quite possible that some of them might perform better. In fact, the indications of the present analysis seem to be that the energy error may depend significantly on the algorithm and that it is a priori very difficult, if not impossible, to establish which performs better. Therefore, a dedicated analysis should probably be repeated case by case.

Of course, a completely different approach should be used, if accuracy, rather than energy conservation, is the issue. In such a case, higher-order algorithms are mandatory. In this respect, it might be interesting to know whether the differences in the energy conservations of the second-order algorithms considered here reflect themselves in the corresponding composition algorithms (see e.g. [5] for a review of composition algorithms).

Our analysis rests on a number of hypotheses, three of which are particularly important. First, we have assumed small integration steps. This is a crucial hypothesis: a second-order analysis cannot say anything about large integration steps. Since large integration steps are a common practice, e.g., in molecular dynamics, this is a severe limitation. In order to gain some insight into the problem one might try to repeat the analysis at order four.

Second, we have chosen to measure the quality of an algorithm, for a given body, from its largest energy error, as a function of the angular momentum. This seems appropriate for situations in which the direction of the angular momentum does not remain confined to a subregion of the unit sphere in the body. If this is not the case, different criteria should probably be used.

Third, we have assumed that the rigid body has a fixed point and that there are no external forces. If there are conservative forces with potential energy V, then the Hamiltonian is

$$H = K + V$$

with K as in (1). Since the exact flow of the potential energy is easily computed, second-order algorithms for Φ_h^H can still be obtained by splitting, e.g.

$$\Psi_h^H = \Phi_{h/2}^V \circ \Phi_h^K \circ \Phi_{h/2}^V \tag{11}$$

(see [4,10] for the computation of Φ_h^V within the "left–trivialized" implementation; when using Euler angles, the computation is trivial [3]). Here, the flow Φ_h^K can be approximated by any of the splitting considered before, SR, RS or 3R: if $\tilde{K}$ is the modified Hamiltonian of the chosen algorithm for Φ_h^K, then $\Phi_h^K = \Phi_h^{\tilde{K}} + \mathcal{O}(e^{-1/h})$ and hence

$$\Psi_h^H = \Phi_{h/2}^V \circ \Phi_h^{\tilde{K}} \circ \Phi_{h/2}^V + \mathcal{O}\left(e^{-1/h}\right).$$

Therefore, by (4), $\Psi_h^H = \Phi_h^{\tilde{H}} + \mathcal{O}(e^{-1/h})$ with modified Hamiltonian

$$\begin{aligned}\tilde{H} &= \tilde{K} + V + \frac{h^2}{12}\left[\left\{\tilde{K} + \frac{1}{2}V, \left\{\tilde{K}, V\right\}\right\}\right] + \cdots \\ &= H + \frac{h^2}{12}\left[\tilde{K}_2 + \left\{K + \frac{V}{2}, \{K, V\}\right\}\right] + \cdots.\end{aligned}$$

Thus, the leading term of the energy error $\tilde{H} - H$ differs from that of the chosen splitting for Φ_h^K in the quantity

$$\frac{h^2}{12}\left\{K + \frac{1}{2}V, \{K, V\}\right\}$$

which is independent of the splitting algorithm for Φ_h^K. Therefore, even if for a specific V everything might happen, it is anyway expected that, in general, the better the algorithm for the kinetic energy, the better the overall algorithm. Completely similar considerations can be made for the case of a rigid body with no fixed point.

Remark. Eq. (11) makes it clear that, as we have mentioned in Section 1, the conjugacy of two algorithms for the Euler–Poinsot system may be lost if these algorithms are used to form a splitted algorithm for a case with external forces. The same consideration applies to the possibility of preprocessing the algorithm for the Euler–Poinsot systems (see [5] for the notion of preprocessing).

Acknowledgements

This work has been done under the auspices, and was partially funded by, the EU Project HPRN-CT-2000-0113 *MASIE—Mechanics and Symmetry in Europe*. The idea of this work originated during several conversations with Ben Leimkuhler. The author thanks him and Ernst Hairer for very useful discussions on these topics, and the referees for very useful remarks. Part of this work was done during a visit of the author at the Section de Mathématique of the Université de Genève, made possible by the financial support of the *Swiss National Science Foundation*, under Grant 20-64954.01.

Appendix A. Extrema of $p(M)$

We prove here that the maximum of the absolute value of the polynomial $p(M)$ on the unit sphere is given either by (9) or by (10).

Lemma. *The nonzero extrema in the first octant of the unit sphere of the polynomial* $p(M) = 4c_1M_2^2M_3^2 + 4c_2M_3^2M_1^2 + 4c_3M_1^2M_2^2$ *are located at some of the following points*:

(i) *The three points*

$$\left(0, \frac{1}{\sqrt{2}}, \frac{1}{\sqrt{2}}\right), \quad \left(\frac{1}{\sqrt{2}}, 0, \frac{1}{\sqrt{2}}\right), \quad \left(\frac{1}{\sqrt{2}}, \frac{1}{\sqrt{2}}, 0\right). \tag{A.1}$$

(ii) *If* $c_1c_2c_3 \neq 0$ *and if the three numbers*

$$k_1 = \frac{c_2 + c_3 - c_1}{c_2c_3}, \quad k_2 = \frac{c_3 + c_1 - c_2}{2c_3c_1}, \quad k_3 = \frac{c_1 + c_2 - c_3}{2c_1c_2}$$

are either all positive or all negative, then also the point

$$\left(\sqrt{\frac{k_1}{k}}, \sqrt{\frac{k_2}{k}}, \sqrt{\frac{k_3}{k}}\right), \tag{A.2}$$

where $k = k_1 + k_2 + k_3$.

(iii) *If one of the coefficients* c_1, c_2, c_3 *vanishes, say* $c_i = 0$, *and the other two are equal to each other,* $c_j = c_k$, *then also all points on the circle* $M_i = 1/\sqrt{2}$, $(i = 1, 2, 3)$.

Proof. Critical points are located at those points at which the gradient $p'(M)$ is parallel to M, that is

$$\begin{pmatrix} (c_2M_3^2 + c_3M_2^2)M_1 \\ (c_3M_1^2 + c_1M_3^2)M_2 \\ (c_1M_2^2 + c_2M_1^2)M_3 \end{pmatrix} = c \begin{pmatrix} M_1 \\ M_2 \\ M_3 \end{pmatrix} \tag{A.3}$$

for some $c \in \mathbb{R}$. We divide the solutions to this equation in several different types:

1. Let us first look for solutions with $M_1 > 0$, $M_2 > 0$, $M_3 > 0$. In such a case, (A.3) is equivalent to

$$A \begin{pmatrix} M_1^2 \\ M_2^2 \\ M_3^2 \end{pmatrix} = \begin{pmatrix} c \\ c \\ c \end{pmatrix}, \quad A = \begin{pmatrix} 0 & c_3 & c_2 \\ c_3 & 0 & c_1 \\ c_2 & c_1 & 0 \end{pmatrix}. \tag{A.4}$$

Since $\det A = 2c_1c_2c_3$ we distinguish two subcases:

1.1. If $c_1c_2c_3 \neq 0$, then (A.4) has the unique solution

$$\begin{pmatrix} M_1^2 \\ M_2^2 \\ M_3^2 \end{pmatrix} = \text{const} \begin{pmatrix} k_1 \\ k_2 \\ k_3 \end{pmatrix},$$

where the normalization factor has to be chosen in such a way that $\|M\| = 1$, that is, $\text{const} = 1/k$ for $k = k_1 + k_2 + k_3$. This solution produces a critical point of the type sought for here if and only if k_1, k_2 and k_3 are all nonzero and have the same sign, as in case (ii)

1.2. If $c_1 = 0$, then (A.3) reduces to

$$c_2M_3^2 + c_3M_2^2 = c, \quad c_3M_1^2 = c, \quad c_2M_1^2 = c.$$

Since $M_1 \neq 0$, the last two equations imply $c_2 = c_3$. But then $c_2 = c_3 \neq 0$ (since otherwise $p(M) = 0$) and hence the first equation gives $M_1^2 = M_2^2 + M_3^2$; together with $M_1^2 + M_2^2 + M_3^2 = 1$ this gives $M_1 = 1/\sqrt{2}$, as in case (iii)

2. We now look for a solution to (A.3) with $M_1 = 0$ but nonzero M_2 and M_3. Eq. (A.3) reduces to

$$c_1M_3^2 = c, \qquad c_1M_2^2 = c. \tag{A.5}$$

When $c_1 = 0$ these equations are satisfied by all M_2 and M_3 (for $c = 0$), so that all points on the circle $M_1 = 0$ are critical points; but if $c_1 = 0$, then $p(M)$ vanishes at all these points, so we do not consider them. If instead $c_1 \neq 0$, then (A.5) lead to $M_2 = M_3 = 1/\sqrt{2}$; thus the point $(0, \frac{1}{\sqrt{2}}, \frac{1}{\sqrt{2}})$ is a critical point of $p(M)$. (For simplicity, in (i) we have formulated this fact without the restriction $c_1 \neq 0$ because, as we have just seen, this point is a critical point also when $c_1 = 0$.)

3. It only remains to look for solutions with $M_1 = M_2 = 0$ and $M_3 = 1$. Since $p'(M)$ vanishes at this point, (0,0,1) is a critical point. However, p vanishes at this point. □

Formulas (9) and (10) are obtained by observing that $p(M)$ attains the values c_1, c_2, c_3 at the three points (A.1) and the value

$$\frac{4}{k^2}(c_1k_2k_3 + c_2k_3k_1 + c_3k_1k_2) = \frac{4c_1c_2c_3}{c_1^2 + c_2^2 + c_3^2 - 2c_1c_2 - 2c_2c_3 - 2c_1c_3}$$

at the point (A.2), if it exists. In case (iii) if $c_i = 0$ and $c_j = c_k$, then $p(M)$ has the constant value c_j at all points of the circle $M_i = 1/\sqrt{2}$.

Appendix B. Regions boundaries

The curve dividing the two SR regions is

$$x = \frac{y}{2-y}, \quad 2 - \sqrt{2} < y < 1,$$

and corresponds to the fact that $\Delta^{\mathrm{SR}}(I_{\max}, I_{\mathrm{mid}}, I_{\min}) = \Delta^{\mathrm{SR}}(I_{\min}, I_{\mathrm{mid}}, I_{\max})$ (namely $|c_2^{\mathrm{SR}}(1, y, x)| = |c_2^{\mathrm{SR}}(x, y, 1)|$). The boundary of the 3R region is union of the two curves

$$x = 2y\frac{y^2 - y + \sqrt{(1 - 4y + 9y^2 - 8y^3 + 2y^4)/2}}{1 - 3y + 4y^2}, \quad 1 > y > y_2 \approx 0.7274$$

and

$$x = y\frac{y^2 - 1 + \sqrt{3 - 6y + 6y^2 - 4y^3 + y^4}}{1 - 2y + 2y^2}, \quad y_2 > y > y_1 \approx 0.6766.$$

Precisely, $y_2 = 1 + \sqrt{(3/8)} - \sqrt{(3/8) + (1/\sqrt{6})}$ and $y_1 = (1/6) - (1/3\alpha) + (\alpha/6)$ for $\alpha = (47 + 3\sqrt{249}/2)^{1/3}$. (The first curve corresponds to the condition $c_2^{\mathrm{SR}}(x, y, 1) = -c_2^{\mathrm{3R}}(1, y, x)$ and the second one corresponds to $c_2^{\mathrm{SR}}(x, y, 1) = c_1^{\mathrm{3R}}(1, y, x)$.)

References

[1] R. Abraham, J.E. Marsden, Foundations of Mechanics, Benjamin, Reading, 1978.
[2] V.I. Arnold, in: Mathematical Methods of Classical Mechanics, Graduate Texts in Mathematics, vol. 60, Springer, New York, 1989.
[3] G. Benettin, A.M. Cherubini, F. Fassò, A "changing chart" symplectic algorithm for rigid bodies and other dynamical systems on manifolds, SIAM J. Sci. Comp. 23 (2001) 1189–1203.
[4] A. Dullweber, B. Leimkuhler, R. McLachlan, Symplectic splitting methods for rigid body molecular dynamics, J. Chem. Phys. 107 (1997) 5840–5851.
[5] E. Hairer, C. Lubich, G. Wanner, Geometric Numerical Integration, Springer, Berlin, 2002.
[6] E. Leimanis, in: The General Problem of the Motion of Coupled Rigid Bodies about a Fixed Point, Springer Tracts in Natural Philosophy, vol. 7, Springer, Berlin, 1965.
[7] J.E. Marsden, T.S. Ratiu, in: Introduction to Mechanics and Symmetry, Texts in Applied Mathematics, vol. 17, Springer, New York, 1994.
[8] R.I. McLachlan, Explicit Lie–Poisson integration and the Euler equations, Phys. Rev. Lett. 71 (1993) 3043–3046.
[9] R.I. McLachlan, P. Atela, The accuracy of symplectic integrators, Nonlinearity 5 (1992) 541–562.
[10] S. Reich, Momentum conserving symplectic integrators, Physica D 76 (1994) 375–383.
[11] J. Touma, J. Wisdom, Lie–Poisson integrators for rigid body dynamics in the solar system, Astr. J. 107 (1994) 1189–1202.